TR－H－014

Numerical Bifurcation Analysis of an Oscillatory Neural Network with Synchronous/Asynchronous Connections

Yukio Hayashi

1993. 7. 16

ATR人間情報通信研究所

〒619-02 京都府相楽郡精華町光台2-2　☎07749-5-1011

ATR Human Information Processing Research Laboratories

2-2, Hikaridai, Seika-cho, Soraku-gun, Kyoto 619-02 Japan

Telephone: +81-7749-5-1011
Facsimile: +81-7749-5-1008

Numerical Bifurcation Analysis of an Oscillatory Neural Network with Synchronous/Asynchronous Connections *

Yukio Hayashi

ATR Human Information Processing Research Laboratories

2-2, Hikaridai, Seika-cho, Soraku-gun, Kyoto 619-02, Japan.

July 15, 1993

Abstract

One of the advantages of oscillatory neural networks is the dynamic link among features by input-dependent synchronization of oscillations.
We have discussed the relation between synchronous/asynchronous oscillation and the connection architectures of an oscillatory neural network with two pairs of excitatory-inhibitory cells. Through numerical analysis, we show synchronous and asynchronous connection types in a wide parameter area for two different inputs and one connection parameter.
The results are not only consistent with the classification of synchronous/asynchronous connection types in Kőnig's model (1991) in the sense of an equivalent self-feedback, but also offer a useful guideline on how to construct a network with local connections for a segmentation task.

*This paper is submitted to Journal of Neural Computation, MIT press.

1 Introduction

Recently, stimulus-specific synchronous oscillations in cat visual cortex have been reported by two research groups in Germany (Eckhorn et al., 1988; Gray et al., 1989). The synchronous oscillations are interesting not only biologically, but also computationally as a dynamic feature-binding mechanism in the brain.

The hypothesis of dynamic feature-binding is that oscillations quickly create dynamic links between synchronized features, which are segmented from desynchronized features for spatial segmentation (Shmizu & Yamaguchi, 1989; Sompolinsky et al., 1991) or temporal segmentation (Wang et al., 1990; Horn et al., 1991; Malsburg & Buhmann, 1992).
However, in order to create a dynamical information synthesis function by synchronization, bifurcation analysis based on different inputs and the influence of the topological connection architecture of an oscillatory neural network on its computational function, should be discussed quantitatively as well as qualitatively.

In a general case of coupled oscillator models with E-I (excitatory-inhibitory) pairs, a theoretical analysis of synchronization is almost impossible. One reason is that the input bias changes not only the number and position of the equilibrium points, but also the characteristic frequencies of the oscillators. In the case of two oscillators without input bias, theoretical analyses of in-phase/anti-phase oscillations have been reported (Kawato & Suzuki, 1980; Nagashino & Kelso, 1991).

Khibnik et al. (1992) have reported a numerical bifurcation analysis similar to that found in this paper. Since the model incorporates the more complex Willson-Cowan oscillators (Borisyuk & Kirllov, 1992), even though they are two homogeneous oscillators with an "identical input bias," the bifurcation routes are very complex. Hopf bifurcation (limit cycle $\leftrightarrow$ torus) is common to each case.

However, the case with different input values is more important to the dynamical information synthesis by synchronizations, because, as feature-binding, we want to create dynamical synchronized clusters at some positions according to the inputs or the relations among them.

Kőnig et al. (1991) have proposed that there are two types of connections on a coupled neural network with different inputs, synchronous and asynchronous. They show that the connection from an E-cell to the nearest-neighbor I-cell causes synchronism, and the connection from an E-cell to the next nearest-neighbor E-cell causes asynchronism. However, their discussion, based on several examples, is merely qualitative. As a guideline to constructing a network for a segmentation task, further quantitative analysis is required.

In this paper, we investigate by numerical analysis the relation between synchronous/asynchronous oscillations and connection architectures in a model with two E-I pairs.

We show that, in a wide parameter area for two different inputs and one connection parameter, the excitatory-excitatory and inhibitory-inhibitory connections between two pairs tend to be asynchronous, while the excitatory-inhibitory and inhibitory-excitatory connections tend to be synchronous. We discuss briefly how to use the results to construct a network with local connections for a segmentation task.

2 Four types of connection architectures

First, we discuss the effect of delay in Kőnig's E-I oscillator, and show that in the case of small delay, the effect of delay is equivalent to that of positive self-feedback. Then we introduce a model without delay but with self-feedback. We are not interested in the result for Wilson-Cowan's model (Borisyuk & Kirllov, 1991) or Kőnig's model per se, but rather in the general behavior for synchronizations of coupled oscillators with E-I connections.

Kőnig's E-I oscillator model is

$$\tau_0 \dot{x}_e(t) = -\alpha x_e(t) - WF(x_i(t-\tau)) + i_e, \quad (1)$$
$$\tau_0 \dot{x}_i(t) = -\alpha x_i(t) + WF(x_e(t-\tau)), \quad (2)$$
$$F(x) = 1/(1+\exp^{\sigma(\theta-x)}). \quad (3)$$

In the above notation, $\dot{x}_i$ denotes the time-differential of the variable x_i.
When the delay τ is small, Kőnig's E-I oscillator in equations (1)-(3) can be approximated to the following linearized equations using $x(t-\tau) \approx x(t) - \tau\dot{x}(t)$ (from a personal discussion paper by Dr. Masa-aki Sato).

$$(\tau_0^2 + \tau^2 W^2 F_e' F_i') \begin{bmatrix} \delta\dot{x}_e \\ \delta\dot{y}_i \end{bmatrix} = \begin{bmatrix} -\alpha\tau_0 + W^2\tau F_e' F_i' & -(\tau_0 + \alpha\tau)WF_i' \\ -(\tau_0 + \alpha\tau)WF_e' & -\alpha\tau_0 + W^2\tau F_e' F_i' \end{bmatrix} \begin{bmatrix} \delta x_e \\ \delta x_i \end{bmatrix}. \quad (4)$$

Here F_e', F_i' are the derivatives $F'(\bar{x}_e), F'(\bar{x}_i)$ at an equilibrium point $\bar{x}_e, \bar{x}_i$.
The eigenvalue of the Jacobian matrix is $\lambda = -\alpha\tau_0 + W^2\tau F_e' F_i' \pm i(\tau_0 + \alpha\tau)W\sqrt{F_e' F_i'}$. When the real-part of λ is positive, $W^2\tau F'(\bar{x}_e)F'(\bar{x}_i) > \alpha\tau_0$, there is a limit cycle. Note that when the delay is small, the effect of the delay is equivalent to that of positive self-feedback.
Thus, in this paper, we consider the effect of positive self-feedback, in various connection architectures.

Next, we consider a model of oscillatory neural networks with two symmetrically connected homogeneous E-I pairs. The four types of connection architectures are shown in Fig. 1. The dynamic equations are as follows ($i, j = 1$ *or* 2, $j \neq i$).

$$(Case\ 1)\quad \dot{x}_i = -x_i + G(W_{ii}x_i - K_{EI}y_i + I_i + W_{ij}x_j), \quad \dot{y}_i = -y_i + G(K_{IE}x_i), \quad (5)$$
$$(Case\ 2)\quad \dot{x}_i = -x_i + G(W_{ii}x_i - K_{EI}y_i + I_i - K_{EI2}y_j), \quad \dot{y}_i = -y_i + G(K_{IE}x_i), \quad (6)$$
$$(Case\ 3)\quad \dot{x}_i = -x_i + G(W_{ii}x_i - K_{EI}y_i + I_i), \quad \dot{y}_i = -y_i + G(K_{IE}x_i - IW_{ij}y_j), \quad (7)$$
$$(Case\ 4)\quad \dot{x}_i = -x_i + G(W_{ii}x_i - K_{EI}y_i + I_i), \quad \dot{y}_i = -y_i + G(K_{IE}x_i - K_{IE2}x_j). \quad (8)$$

Each x_i and y_i are an excitatory and inhibitory cells, respectively. $G(z)$ is a sigmoid function; $G(z) = 2\arctan(z/a)/\pi$ and a is the slope of $G(z)$. The connections for each E-I pair are: self-excitatory, W_{ii}; inhibitory, $-K_{EI}$; and excitatory, K_{IE}. The connections have the same constant values independent of the cell number i. These values are set to $W_{ii} = 1.0$, $K_{IE} = K_{EI} = 2.0$, $a = 0.1$, to satisfy the oscillatory condition of an E-I pair (Hayashi, 1992).
The symmetrical connections between E-I pairs are: excitatory, W_{ij} (Case 1) or K_{IE2} (Case 4); inhibitory, $-K_{EI2}$ (Case 2) or $-IW_{ij}$ (Case 3), respectively. I_i is the input bias for the i-th excitatory cell ($I_1 \neq I_2$). These variables I_i and W_{ij} (or $K_{EI2}, IW_{ij}, K_{IE2}$) are bifurcation parameters.

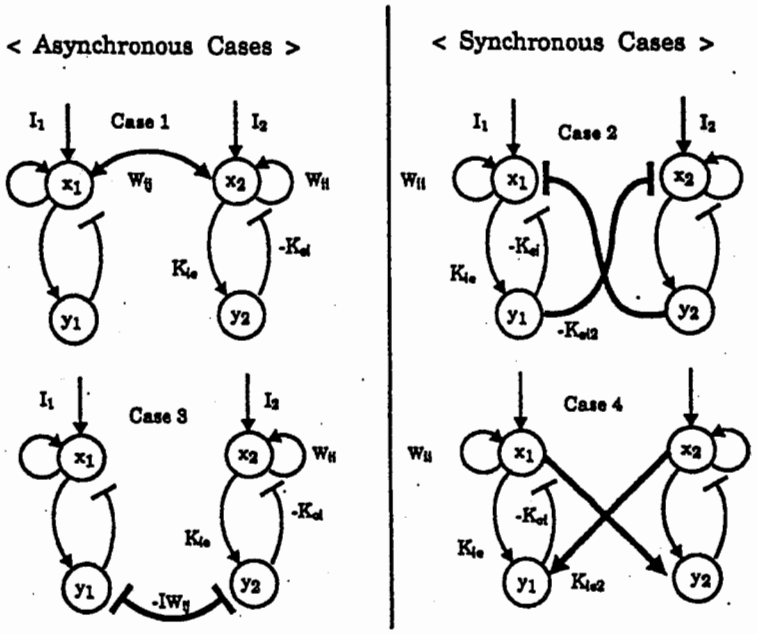

Figure 1: Four types of connection architectures. Symmetrical connections between homogeneous E-I pairs (excitatory cell: x_i, inhibitory cell: y_i, input bias: I_i) are denoted by a bold-line. $\dashv$ and $\rightarrow$ denote inhibitory connections and excitatory connections, respectively.

3 Results of numerical analysis

In this section, we show by numerical analysis that Cases 1 and 3 tend to be asynchronous, while Cases 2 and 4 tend to be synchronous over a wide parameter area. We also explain briefly the differences between the bifurcation structures of the four cases.
We define the synchronous and asynchronous oscillations as a frequency-locking limit cycle and a frequency-unlocking quasi-periodic orbit or chaos, respectively.

First, the two input biases are assumed to be $I_1 > 0, I_1 > I_2$. Each input is varied from -1.0 to 1.0 in 0.2 increments. By exchange of cell numbers, $I_1 < I_2$ is equivalent to the case $I_1 > I_2$, and by simple variable-change ($\tilde{x}_i = -x_i, \tilde{y}_i = -y_i, \tilde{I}_i = -I_i$) using the fact that $G(z)$ is an odd function, the case $I_1 < 0$ is also equivalent to the case $I_1 > 0$. Thus, the result has symmetry.

For a combination of the input bias, each connection parameter is varied from 0.01 to 2.6 in 0.001 increments. On the 4-th order Runge-Kutta approximation ($\Delta t = 0.01$), there are 30,000 iterations after 30,000 iterations of the transition phase from the initial values: $x_i(0) \equiv I_i$, $y_i(0) \equiv 0$. Though the model has multi-stable solutions for different initial states from the conditions $x_i(0) \equiv I_i, y_i(0) \equiv 0$, only the case of the above initial states is discussed below.

We obtained the bifurcation diagrams according to whether the oscillations are frequency-locked or not, using Fourier analysis of the waveform $x_i(t)$ and a Poincaré section on the projection planes $x_i - y_i$. In this paper, we do not discriminate between chaos and a quasi-periodic orbit.

Fig. 2 shows each 3D diagram that has a roof on the start points of stable points by the primary Hopf bifurcation, and a curved surface on the start points of harmonic limit cycles by frequency locking from quasi-periodic orbits. Fig. 3 shows the 2D-sections of $I_1 = const$ for each case. In the figure, (α, β) denotes the winding numbers of a harmonic limit cycle on each projection plane.

The main result of this paper is the following.
For the HLC regions in the weakly connected area (0 < each connection parameter < 1) under the roof, the difference between Cases 1 & 3 and Cases 2 & 4 is as follows.

(Cases 1 and 3) Since there are only several thin, isolated HLC regions in the wide QPO region, the oscillations between E-I pairs with different input biases tend to be asynchronous.

(Cases 2 and 4) Since the QPO region is comparatively small in the SLC and HLC regions, the oscillations tend to be synchronous . The harmonics (1, 2), (2, 2) and simple limit cycle coexist in the HLC regions.

In Cases 1 and 3, the thin HLC regions are not drawn in the left and right wings of the QPO region, because the figures have symmetry. When the input bias I_1 is less than 0.8 in Case 3, the HLC region of the harmonics (3, 4) vanish, although this is not shown in Fig. 3.
Unfortunately, we can not analytically show this difference between Cases 1 & 3 and Cases 2 & 4. For non-perturbative coupling, a theoretical analysis of the difference in measure of locking regions is very difficult (perhaps even impossible at present). The investigation of the difference requires further study.

In addition, we show other results as follows.
In the strongly connected area, the primary Hopf bifurcation points are approximately on a line (Case 1:W_{hopf} and Case 2: K_{hopf}), or are almost constant (Case 3 : IW_{hopf} and Case 4: K_{hopf}). Though this line can be approximately analyzed, it is not disussed in this paper.

As each connection parameter increases from zero, the common typical bifurcation route is: two independent limit cycles $\rightarrow$ harmonic limit cycle (frequency locking or unlocking by saddle-node birth-death bifurcation on a Poincaré section) $\leftrightarrow$ quasi-periodic orbit (secondary Hopf bifurcation) or chaos (breaking T^2 torus) $\rightarrow$ simple limit cycle (primary Hopf bifurcation) $\rightarrow$ stable point.

Fig. 4(a) shows an example of a typical bifurcation route from torus to stable point through the limit cycle in each case. However, Fig. 4(b) shows an example of a complex bifurcation route from the CM region to the SP region in Cases 2 and 4. As shown in Fig. 4(b), the CM region has a simple limit cycle of the two synchronized pairs, a limit cycle on a line by another destabilized pair and a complex orbit. To determine this complex orbit by type of attractor, a more detailed analysis will be required.

4 Discussions

In the following, we discuss briefly how to use the bifurcation diagrams to construct a network with local connections for a segmentation task.
Based on the result of the bifurcation diagrams of two E-I pairs, we investigated an example of orientation feature extraction from a pattern image of a hand-written number (Hayashi, 1993). In order to synchronize the line segment pixels (corresponding to the E-I pairs) with similar input values in one direction on the drawing, the connection parameter W_{ij} between the nearest-neighbor E-cells (Case 1) in the same direction is set to a value in the synchronous area of the bifurcation diagram. As a result, the synchronizations grow larger than the size of the nearest-neighbor connections, and the power of the cross-correlation between them increases with the increasing value of the connection parameter. Also, the synchronization between pixels depends on the difference in input values. In the case of other connection architectures (Cases 2-4), there is a similar tendency toward synchronization.

These results suggest that, in the case of multi-pairs with local connections, the synchronous area in the parameter area has a qualitatively similar range. However, since such a nonlinear system

is not additive, the general case of multi-pairs (without local connections) may not have a similar result. For the case of multi-pairs, future studies, both theoretical and numerical, are required. The existence of chaos is also an open question (even in the case of two pairs).

In this paper, while the initialization of the states at each input time is assumed, the model has multi-stable solutions for initial states that differ from our conditions $x_i(0) \equiv I_i, y_i(0) \equiv 0$. This is interesting from a theoretical point of view. However, from an application point of view, multi-solutions may be too complex to use for a segmentation task.

5 Conclusion

We have discussed the relation between synchronous/asynchronous oscillations and the connection architectures between two E-I pairs. Through numerical analysis, we have shown that, in a wide parameter area, the excitatory-excitatory and inhibitory-inhibitory connections tend to be asynchronous, while the excitatory-inhibitory and inhibitory-excitatory connections tend to be synchronous.

To conclude, the results are consistent with the classification of synchronous/asynchronous connection types in Kőnig's model in the sense of an equivalent self-feedback. Our analysis indicates that the self-feedback effects are important for this relation between connection types and synchronization of oscillations. Further, we have discussed how our results may be useful for constructing a network with local connections for a segmentation task.

References

[1] Borisyuk, R. M & Kirllov, A. B. (1992). Bifurcation analysis of a neural network model. *Biological Cyberetics*, 66, 319-325.

[2] Eckhorn, R., Bauer, R., Jordan, W., Brosch, M., Kruse, W., Munk, M. & Reitboeck, H. J. (1988). Coherent oscillations: A mechanism of feature linking in the visual cortex? - multiple electrode and correlation analysis in the cat -. *Biological Cybernetics*, 60, 121-130.

[3] Gray, C. M. & Singer, W. (1989). Stimulus-specific neuronal oscillations in orientation columns of cat visual cortex. *Proc. Natl. Acad. Sci. USA*, 86, 1689-1702.

[4] Hayashi, Y. (1992). Learning of Continuously Transformed Pattern Cycles by an Oscillatory Neural Network. *Proc. of IJCNN '92, Baltimore.*

[5] Hayashi, Y. (1993). Dependency of the Connection Architectures of Oscillatory Neural Networks on Synchronization, *Submitted to IJCNN '93, Nagoya.*

[6] Horn, D., Sagi, D. & Usher, M. (1991). Segmentation, Binding, and Illusory Conjunctions. *Neural Computation*, 3(4), 510-525.

[7] Kawato, M. & Suzuki, R. (1980). Two Coupled Neural Oscillators as a Model of the Circadian Pacemaker. *J. Theor. Biol*, 86, 547-575.

[8] Khibnik, A. I, Borisyuk, R. M. & Roose, D. (1992). Numerical bifurcation analysis of a model of coupled neural oscillators. *International Series of Numerical Mathematics*, 104.

[9] Kőnig, P. & Schillen, T. B. (1991). Stimulus-dependent assembly formation of oscillatory responses: I. synchronization and II. desynchronization. *Neural Computation*, 3(2), 15-177.

[10] Nagashino, H. & Kelso, J. A. (1991). Bifurcation of Oscillatory Solutions in A Neural Oscillator Network Model. *Proc. of The Second Symposium on Nonlinear Theory and its Applications*, July 15-17, 119-122.

[11] Shimizu, H. & Yamaguchi, Y. (1989). How Animals Understand the Meaning of Indefinite Information from Environments ?. *Progress of Theoretical Physics Supplement*, (99), 404-424.

[12] Sompolinsky, H., Golomb, D & Kleinfeld, D. (1991). Phase Coherence and Computation in a Neural Network of Coupled Oscillators. *In H. G. Schuster (Eds), Nonlinear Dynamics and Neuronal Networks - Proceedings of the 63rd W. E. Heraeus Seminar Friedrichsdorf 1990 -, (pp. 113-130). VCH.*

[13] von der Malsburg, C., P. & Buhmann, J. (1992). Sensory segmentation with coupled neural oscillators. *Biological Cybernetics*, 67, 233-242.

[14] Wang, D., von der Malsburg, C., P. & Buhmann, J. (1990). Pattern Segmentation in Associative Memory. *Neural Computation*, 2(1), 94-106.

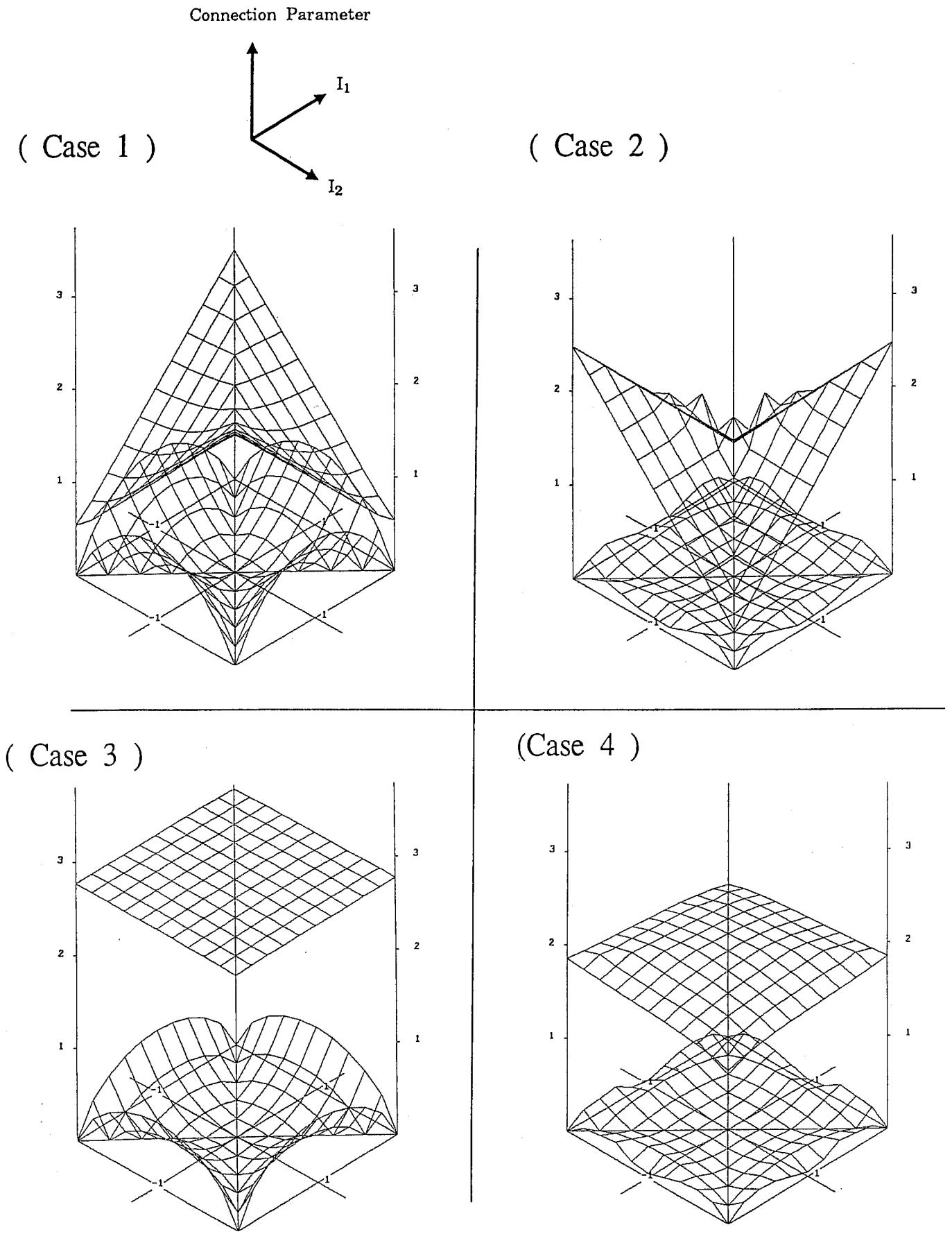

Figure 2: Three-dimensional bifurcation diagram for each case. The roof and the curved surface denote starting points of stable points and harmonic limit cycles, respectively.

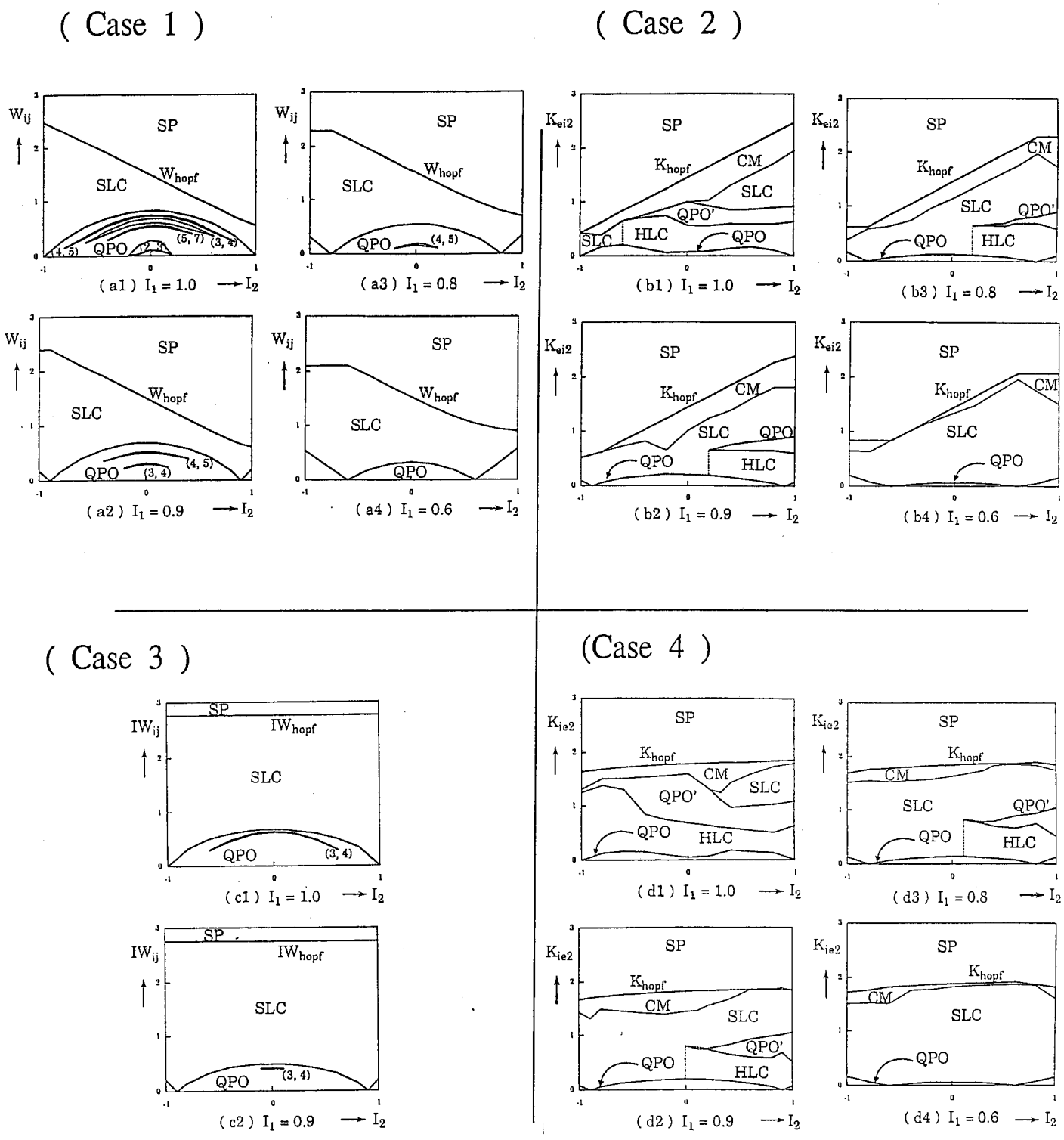

Figure 3: 2D-sections of each diagram ($I_1 = const$). The regions are: SP, stable point; SLC, simple limit cycle; HLC, harmonic limit cycle; QPO, quasi-periodic orbit or chaos from two independent limit cycles; QPO', quasi-periodic orbit or chaos between the SLC and HLC regions; CM, complex mix-mode.

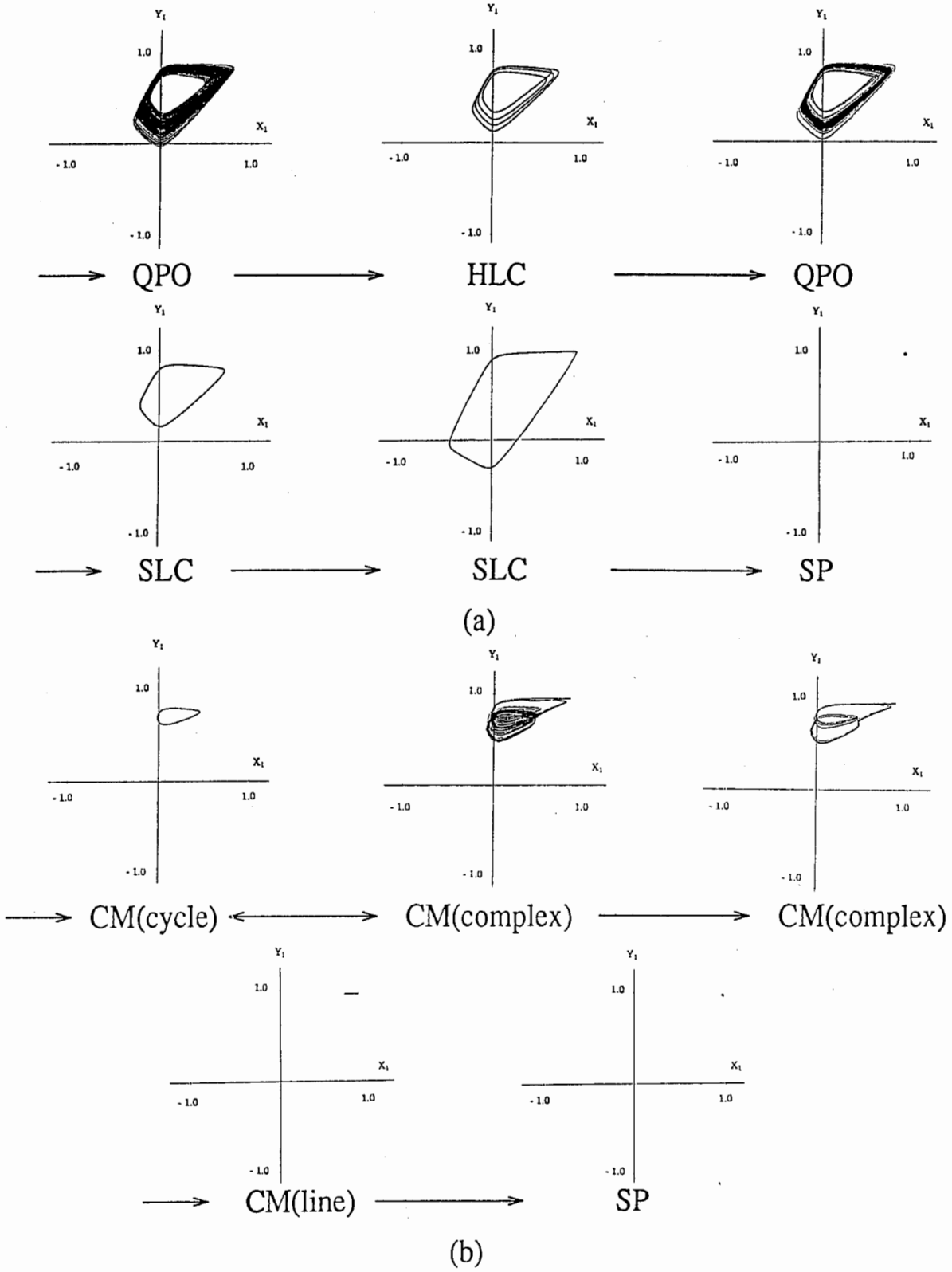

Figure 4: Trajectories on the projection plane $x_1 - y_1$. (a) Typical bifurcation route: QPO - locking $\rightarrow$ HLC - unlocking $\rightarrow$ QPO - 2ndHopf $\rightarrow$ SLC - 1stHopf $\rightarrow$ SP, (b) Complex route: CM(simple limit cycle) $\leftrightarrow$ CM(complex orbit) $\rightarrow$ CM(limit cycle on line) - 1stHopf $\rightarrow$ SP.